MDPI

Article

FEL pulse duration evolution along undulators at FLASH

Mahdi M. Bidhendi [1,*], Ivette J. Bermudez Macias [1,†], Rosen Ivanov [1,†], Mikhail V. Yurkov [1] and Stefan Düsterer [1,*]

[1] Deutsches Elektronen-Synchrotron DESY, Notkestr. 85, 22607 Hamburg, Germany
* Correspondence: mahdi.mohammadi-bidhendi@desy.de, stefan.duesterer@desy.de
† Current address: European XFEL GmbH, Holzkoppel 4, D-22869 Schenefeld, Germany

Abstract: Self-amplified spontaneous emission (SASE) free-electron lasers (FELs) deliver ultrashort pulses with femtosecond duration. Due to the fluctuating nature of the radiation properties of SASE FELs, characterizing the FEL pulses on a single shot basis is necessary. Therefore we use terahertz streaking to characterize the temporal properties of ultra-short extreme ultraviolet pulses from the free electron laser in Hamburg (FLASH). In this study, the pulse duration as well as the pulse energy are measured in a wavelength range from 8 to 34 nm as function of undulators contributing to the lasing process. The results are compared to one-dimensional and three-dimensional, time-dependent FEL simulations.

Keywords: free-electron lasers; temporal diagnostic; XUV pulses; SASE; THz streaking

Citation: M. Bidhendi, M.; Bermudez Macias, I.; Ivanov, R.; Yurkov, M.; Düsterer, S. FEL pulse duration evolution along undulators at FLASH. *Appl. Sci.* **2022**, *1*, 0. https://doi.org/

Received:
Accepted:
Published:

Publisher's Note: MDPI stays neutral with regard to jurisdictional claims in published maps and institutional affiliations.

1. Introduction

The electron bunches in single pass high gain free electron lasers (FEL) propagate through the undulators just once producing the most intense extreme ultraviolet (XUV) and x-ray pulses. The amplification mechanism is the so-called Self Amplification of Spontaneous Emission (SASE) resulting in fundamental statistical fluctuations of the radiation properties. Properties of the radiation pulse energy and the radiation pulse duration have been studied theoretically and experimentally in the last decades for the XUV and x-ray range [1–4]. It turns out that the pulse energy (i.e. number of photons in one ultrashort pulse) grows gradually by many orders of magnitude in the amplification process, whereas the pulse duration first decreases in the exponential stage of amplification, and then grows by about a factor of 2 when the amplification process enters the nonlinear regime.

The evolution of the pulse energy along the undulators, the so-called gain curve, has been measured frequently in the past [5–11]. However, to our knowledge, there has been only one study that investigates the pulse duration in relation to the number of undulators contributing to the lasing [4]. In this study, however, the pulse duration is only estimated by analyzing spectral fluctuations for one x-ray wavelength. Here, we present a more comprehensive study where we measured the single shot pulse duration as well as the pulse energy for six different wavelengths at the FLASH2 facility [11]. In addition to the average, we can analyze the single-shot data and provide experimental values for the shot to shot fluctuations. To get a complete picture of the process, the experimental data are compared FEL simulations.

2. SASE FEL amplification process

The amplification process in SASE FELs develops from the shot noise in the electron beam, passes an exponential stage of amplification, and finally evolves in the nonlinear regime. Figure 1 shows the evolution of the radiation pulse energy and its fluctuations, and the evolution of the radiation pulse duration along the undulator. The results are obtained by the time-dependent FEL simulation code FAST using 1D and 3D FEL models [12]. To be specific, we consider the case of an electron beam with a longitudinal Gaussian profile with an rms duration τ_{el}. Fluctuations of the radiation pulse energy reach a maximum value in

the end of the exponential gain regime and subsequently decreases in the nonlinear regime while the radiation pulse energy continues to grow. In the high gain exponential regime the number of modes M in the radiation pulse is defined as the inverse squared deviation of the radiation pulse energy, $M = 1/\sigma_E^2$, where $\sigma_E^2 = \langle (E_r - \langle E_r \rangle)^2 \rangle / \langle E_r \rangle^2$ [2,13]. The saturation point corresponds to the maximum brilliance of the radiation [14,15]. At the same time the fluctuations of the radiation pulse energy decrease by a factor of 3 with respect to the maximum value. In the framework of the one dimensional model the saturation length and coherence time at saturation

$$z_{sat} \simeq \frac{\lambda_W}{4\pi\rho}\left(3 + \frac{\ln N_c}{\sqrt{3}}\right), \quad (\tau_c)_{max} \simeq \frac{1}{\rho\omega}\sqrt{\frac{\pi \ln N_c}{18}}, \tag{1}$$

are expressed in terms of the FEL parameter ρ [16] and the number of cooperating electrons $N_c = I/(e\rho\omega)$ [2,13,17]. Here ω is the radiation frequency, I is the beam current, $-e$ is the charge of electron, and λ_W is undulator period.

A practical estimate for the parameter ρ comes from the observation that in the parameter range of SASE FELs operating in the VUV and x-ray wavelength range, the number of field gain lengths to reach saturation, is about 10 [14]. Thus, the parameter ρ and the coherence time τ_c relate to the saturation length as:

$$\rho \simeq \lambda_W / z_{sat}, \quad \tau_c \simeq \lambda z_{sat} / (2\sqrt{\pi} c \lambda_W). \tag{2}$$

For the number of modes $M \gtrsim 2$, the rms electron pulse length τ_{el} and the minimum radiation pulse length τ_{ph}^{min} given in FWHM in the end of the exponential gain regime are given by [3,18,20] :

$$\tau_{ph}^{min}(FWHM) \simeq \tau_{el} \simeq \frac{M\lambda}{5\rho} \simeq \frac{M\lambda z_{sat}}{5c\lambda_W}. \tag{3}$$

The minimum radiation pulse duration expressed in terms of coherence time eq. 2 is

$$\tau_{ph}^{min}(FWHM) \simeq 0.7 \times M \times \tau_c. \tag{4}$$

The radiation pulse duration is mainly defined by the length of the lasing fraction of the electron bunch with some corrections related to the slippage effect. In the beginning of the amplification process, the radiation pulse shape just repeats the longitudinal shape of the electron bunch. In the exponential high gain regime the power amplification (and beam bunching) is stronger for higher currents, thus the radiation pulse duration is reduced as the electron bunch travels along the undulator. When the amplification approaches saturation (full bunching) in the central part of the bunch, the tails of the electron bunch begin to contribute more to the radiation power. Beam bunching continues to grow there and the radiation pulse duration starts to grow as well. The effect of the lasing tails gives the same relative radiation pulse lengthening as is illustrated in Fig. 1. The pulse length at the saturation point is about a factor of 1.4 higher than the minimum pulse for the linear regime given by eq. (2), and it is increased further up to about a factor of 2 in the deep nonlinear regime. The second effect leading to pulse lengthening is the slippage of the radiation, by one radiation wavelength per one undulator period. Evidently, the slippage effect is more pronounced for shorter pulses and longer wavelengths.

The case of "cold" (zero energy spread) and monoenergetic electron bunches has been analyzed in earlier papers in the framework of a 1D FEL model [2,3,19,20]. Using the normalized electron pulse duration $\bar{\tau}_{el} = \rho\omega\tau_{el}$ allows to describe the simulation results in a universal way for $\bar{\tau}_{el} \gtrsim 2$. The simulation results normalized this way, show almost identical behavior for different $\bar{\tau}_{el}$ as illustrated in Fig. 1. Note that for $\bar{\tau}_{el} \gtrsim 2$, $\bar{\tau}$ is essentially equal to the number of radiation modes ($\bar{\tau}_{el} \sim M$) [3,20]. In this paper we extend the analysis of short pulse effects using the results of three-dimensional, time dependent simulations carried out with the FAST code. The bold curves in Fig. 1 refer to the 3D simulations applying typical FLASH2 experimental conditions: electron energy 1 GeV, rms energy spread 0.2 MeV and rms normalized emittance 1.4 mm-mrad. The lasing

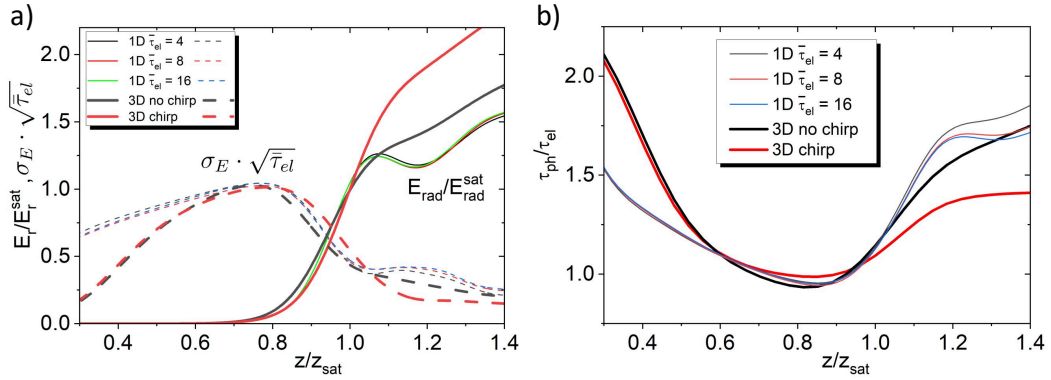

Figure 1. a) Simulated average radiation pulse energy and fluctuations of the radiation pulse energy along the undulator length normalized to the saturation length. The fluctuations are scaled with $\sqrt{\bar{\tau}_{el}}$ to compensate the pulse duration dependence as described below in the text. b) Simulated evolution of the radiation pulse duration along the undulator length. Thin curves show the result of the 1D model for three different electron pulse length $M \sim \bar{\tau}_{el} = 4, 8$ and 16. The black bold curve shows the 3D model for the pulse length of $M \sim \bar{\tau}_{el} = 5$ without energy chirp, and the bold red curve shows the 3D model including energy chirp.

fraction of the electron bunch is approximated with a Gaussian distribution of 16 fs rms pulse duration and 1.5 kA peak current resulting in a radiation wavelength of 13.5 nm. These parameters correspond to the value of $M \sim \bar{\tau}_{el} = 5.1$. Results of the simulations are presented with the same normalization procedure as for the 1D case. The first set of simulations refers to the case of a monoenergetic electron beam (bold black curves). We see that the 1D and 3D results for the monoenergetic case are rather similar starting from the end of the high gain exponential regime. The difference in the linear regime reflects the spatial mode competition effect which is absent in the 1D model. However, at the end of the high gain linear regime the fundamental TEM_{00} FEL mode is significantly larger as compared to other higher spatial modes, and we see a good agreement of the results of the 1D and 3D model.

In the real accelerator the electron beam is not monoenergetic. The long pulse, low current electron beam produced in the electron gun at FLASH is compressed in several stages by a large factor (up to about one hundred), and the peak current is increased correspondingly [21]. To achieve such a large compression, an energy chirp along the electron bunch is applied in the accelerating sections. This energy chirp leads to a bunch compression while the electron bunch moves through dedicated magnetic bunch compressors. An RF induced energy chirp can be minimized such that it only slightly changes FEL properties with respect to a monoenergetic beam. Still, different kinds of wakefields and collective effects in the electron beam generate an energy chirp along the electron bunch. An example of such an energy chirp induced by the longitudinal space charge field (LSC) is shown in Fig. 2 [21]. An important feature of a LSC wake is that the energy of electrons in the lasing fraction of the electron bunch is increased from the tail to the head of the electron bunch. Such a feature leads to a visible increase of the FEL efficiency in the nonlinear regime which on the other hand leads to an increase of the FEL radiation bandwidth. During the experiments discussed in this paper the beam formation system has been tuned such that the LSC produced a significant chirp of about 5 MeV peak-to-peak, resulting in the increase of the radiation spectrum bandwidth by about a factor of two with respect to natural FEL bandwidth. Results of the simulation including the LSC chirped electron beam are shown in Fig. 1 as red bold line. While there is no difference between the chirped and monoenergetic (unchirped) cases in the linear regime, we see visible differences in the post saturation regime. The pulse duration becomes shorter and the radiation pulse energy grows faster in the chirped case. The explanation of this phenomenon can be found in the positive energy chirp along the lasing fraction of the bunch (see Fig. 2) which is equivalent

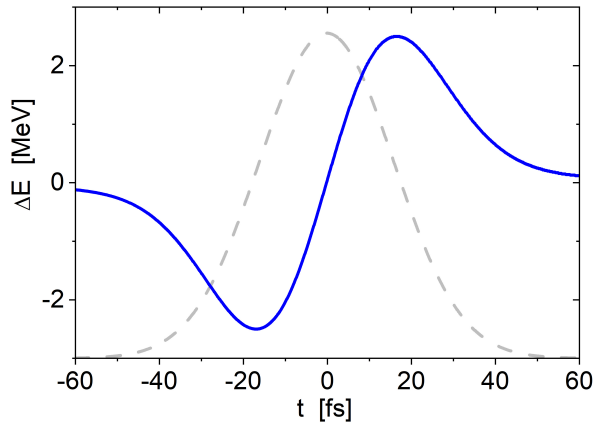

Figure 2. Energy chirp along electron bunch induced by the longitudinal space charge field (blue curve) as it was used for the chirped 3D simulation. The grey dashed curve shows the longitudinal profile of the electron bunch.

to an undulator tapering. Thus, electrons interact more strongly with the radiation and the power grows faster while the radiation pulse duration remains nearly constant. Only the fraction of the bunch radiates where electrons were trapped in the regime of coherent deceleration and in addition the slippage effect is also suppressed.

In the following sections we compare experimental results with the 3D simulations performed for a chirped electron beam. The energy chirp along the lasing fraction of the bunch was set to 150 keV/fs (Fig. 2) leading to a spectral width of about 1% for the XUV pulse in agreement with several spectral measurements performed at FLASH [5,22–24]. The chirp in the electron bunch leads to a chirp of 30 meV/fs in the 13.5 nm XUV pulse or expressed as second order dispersion it yields a value of 25 fs^2, which is comparable to the measurements described in Ref. [25] with a second order dispersion of 50 fs^2, where an exceptionally large bandwidth (i.e. chirp) was requested.

3. FEL measurements

In order to measure the pulse duration of the XUV FLASH pulses, we used the terahertz streaking technique [26–28]. In short, this method is based on photoionization of noble gas atoms in the presence of a strong terahertz (THz) field. If the generated electron wave packet is shorter than half the streaking field period, the temporal structure of the wave packet will be mapped onto the kinetic energy distribution of the emitted electrons and can thus be used to determine the XUV pulse duration. The measurements were performed at the dedicated photon diagnostic beamline FL21 in the FLASH2 branch, which is equipped with a permanently installed THz streaking setup [29]. The setup consists of the interaction chamber containing a time-of-flight spectrometer, a dedicated laser system delivering about 1 ps long pulses at 1030 nm with pulse energy of 3.5 mJ at a repetition rate 10 Hz and a THz generation setup based on optical rectification using a nonlinear crystal ($LiNbO_3$) (for details see e.g. [30,31]).

In Ref. [31] it was discussed that there is an optimum number of photoelectrons created in the ionization process by the FEL pulse. One needs sufficiently many electrons to record a single-shot photoelectron spectrum while limiting the number of electrons so that the resulting space charge effects are negligible. For our setup this leads to an optimum XUV pulse energy in the range of several hundred nJ to few μJ depending on the wavelength for neon as the target gas. To ensure the same experimental conditions for all measurements, the streaking setup was left unchanged during the gain curve measurements while the transmission of a variable XUV attenuator [32] was adapted such that the average number of created photoelectrons was constant for each measured setting.

FLASH2 is equipped with 12 variable gap undulator segments, each of 2.5 m length and 31.4 mm period [11]. The pulse duration was measured with the streaking setup

while varying the number of undulators contributing to the lasing. The shown data results from 3 different measurement campaigns. In the first one, FLASH2 was set to 3 different wavelengths: 8, 12 and 16 nm with a constant electron bunch energy of 1.00 GeV and an electron bunch charge of 0.19 nC leading to XUV pulse durations on the order of 100 fs FWHM. For the second campaign the FLASH2 electron bunch energy was 875 MeV with a bunch charge of 0.2 nC, and the wavelength was set to 10 and 20 nm leading to XUV pulse durations ranging from 50 to 160 fs FWHM. Besides these two campaigns, the third campaign was performed with a significantly lower electron bunch energy of 434 MeV, electron bunch charge of 0.2 nC leading to a wavelength of 34 nm. The experimental results are summarized in table 1.

Table 1. Main parameters derived from the measurements shown in Fig. 3. The values are deduced from scaling the experimental data to the 3D simulation. With z_{sat} as saturation length in "number of undulators" with a maximum number of undulators of 12 at FLASH2, $\tau_{ph}^{min}(FWHM)$ as minimum pulse duration, and E_{sat} as the saturation pulse energy. In order to compare the experimental data to the 1D simulation, the normalized electron pulse duration $\bar{\tau}_{el}$ (equivalent to the number of modes M) was determined for all measured wavelengths using Eq. 4 and the coherence time at saturation τ_c^{sat} (FWHM) was taken from Refs. [20,33].

Wavelength	**electron bunch energy**	z_{sat}	$\tau_{ph}^{min}(FWHM)$	E_{sat}	$\tau_c^{sat}(FWHM)$	$\bar{\tau}_{el}\|M$
8 nm	1008 MeV	9.4	75 fs	60 μJ	7fs	22
10 nm	875 MeV	8.9	50 fs	39 μJ	8 fs	13
12 nm	1008 MeV	7.7	88 fs	88 μJ	9 fs	16
16 nm	1008 MeV	7.0	105 fs	130 μJ	12 fs	16
20 nm	875 MeV	6.1	95 fs	50 μJ	15 fs	13
34 nm	434 MeV	8.3	77 fs	26 μJ	20 fs	8

For all measurements except at 34 nm, the undulators were not tapered (all undulators contributing to the lasing had the same gap settings i.e. the same K-value), in order to compare the experimental values with the simulations. For each wavelength, the pulse duration was first measured when all 12 undulators were closed (thus all undulators contributing to the lasing). Afterward, starting with the undulators closest to the experiments, one pair of undulators at a time was opened until no measurable XUV pulse energy could be detected. Since only the down stream undulators were opened, the trajectory in the first (lasing) undulators was kept constant. The resulting shift of the source point of the XUV radiation enlarges the XUV focal spot in the streaking interaction region slightly, however it is still sufficiently smaller (< 300 μm FWHM) as compared to the THz focal spot (~ 1 mm FWHM) and did not lead to significant changes for the THz streaking measurements. The energy of the XUV pulses was simultaneously measured with an absolutely calibrated pulse energy detector (GMD) [34] provided by the FLASH photon diagnostic.

4. Discussion

We analyzed the average pulse energies and average pulse durations as well as their respective fluctuations as function of the number of undulators contributing to the lasing process for six different wavelengths. As basis we used the 3D simulation based on the chirped electron bunch. In the first step the number of undulators was scaled to the undulator coordinate z, such that the onset of measurable SASE (> 0.5 μJ) coincides with the z range in which the energy gain becomes visible in the simulated energy gain curve ($z/z_{sat} \sim 0.7$). This determines the undulator axis scaling and already fixes the saturation length z_{sat}. It has to be noted that we took into account that the first two undulator segments at FLASH2 hardly contribute to the lasing due to the slight misalignment and thus we counted the first 2 undulators as 0.5 undulators (i.e. subtracting 1.5 from the actual number of closed undulators). In the second step the pulse energy was scaled such that the pulse

energy at saturation length $z = z_{sat}$ was defined as saturation pulse energy E_{sat} and all energies were normalized by the saturation energy. A similar normalization was applied for the pulse duration. Here, the measured values were scaled to the minimum pulse duration τ_{min} at $z/z_{sat} \sim 0.8$. It is important to note that the experimental data has been only rescaled and not fitted to the simulation result.

Fig. 3 shows the experimentally measured pulse duration (red spheres) as well as the 3D simulation including chirp (red line) and the 3D simulation without chirp (red dashed lines). The 3D model without chirp predicts a considerable pulse lengthening when the amplification process enters the nonlinear regime (similar to the 1D models as shown in Fig. 1), while the chirped simulation shows clearly less pulse lengthening. The experimental pulse duration data does also not indicate a strong lengthening of the XUV pulses in saturation and thus shows a good agreement with the 3D simulation including chirp. For the pulse energy we measure a steady increase in saturation and beyond. This behavior is again well represented by the 3D model including chirp, while the 3D model without chirp predicts less energy increase after the saturation point.

The pulse energies as well as the pulse durations are stochastically fluctuating due to the SASE process and fluctuations induced by the acceleration process as well as measurement uncertainties in the actual THz streaking measurement [20], leading to a broad distribution. Example histograms of the fluctuations measured for a specific setting (fixed wavelength and number of undulators) are shown in Fig. 4 b) and d). The rms value of the fluctuations are also used as "error bars" in Fig. 3 denoting not the measurement uncertainty but showing the range of the measured values. The actual experimental uncertainty for single shot measurements was determined to be about ±20% for the pulse duration measurements [31] and about ±10% for the pulse energy measurements [20], thus only a small fraction of the shown "error bars" of the averaged values result from the measurement uncertainties.

In Fig 4 a) and c), the normalized fluctuations are presented as function of z. The fluctuations are not constant along the amplification process and for fewer closed undulators the fluctuations are much larger. Both the 1D and 3D simulations show that for pulse duration and pulse energy the relative fluctuations are largest in the linear regime and are decreasing strongly in the range of z/z_{sat} 0.8 to 1 and only decrease slowly after saturation is reached.

In contrast to the simulated values of the pulse energy and the pulse duration (Fig. 1) which are essentially pulse length independent, the respective fluctuations are indeed pulse duration dependent. We know from Ref. [20] that the fluctuation of pulse duration and pulse energy is inversely proportional to the square root of the number of modes as is also indicated by the scaling in Fig. 1 a). Therefore we expect less fluctuations for longer pulses (i.e. larger number of modes), as can be seen in Fig. 4 a) and c). To compare the fluctuations predicted from the 1D and 3D model, the number of modes should be in the same range. As the number of modes used for the 3D simulation is 5.1, therefore we can compare it to the 1D simulation with 4 and 8 number of modes ($\bar{\tau}_{el} = 4$ and $\bar{\tau}_{el} = 8$). The result shows that the 3D simulation lays between the 1D simulation with 4 and 8 number of modes. Most measured XUV pulse durations were significantly longer ($\bar{\tau}_{el}$ in the range of 15-20 as shown in table 1) and thus can be compared to the 1D simulation with $\bar{\tau}_{el} = 16$. The experimental values show essentially the same trend as the 1D simulation with $\bar{\tau}_{el} = 16$, with however significantly higher fluctuations as the simulation predicts. This observation was already described in [20] and can be attributed to additional fluctuations in the accelerator and measurement uncertainties besides the SASE inherent fluctuations.

An interesting property for experiments is the radiation power (pulse energy divided by the pulse duration). In Fig. 5 a) we compare how the power scales with z. It turns out that the achievable power of the FEL pulses increases for all experimental settings continuously along the undulators, even in saturation without a hint for a local maximum. The chirped 3D simulation predicts the same behavior and shows a very good agreement with the experimental data. The non-chirped 3D simulations exhibit a similar trend in the

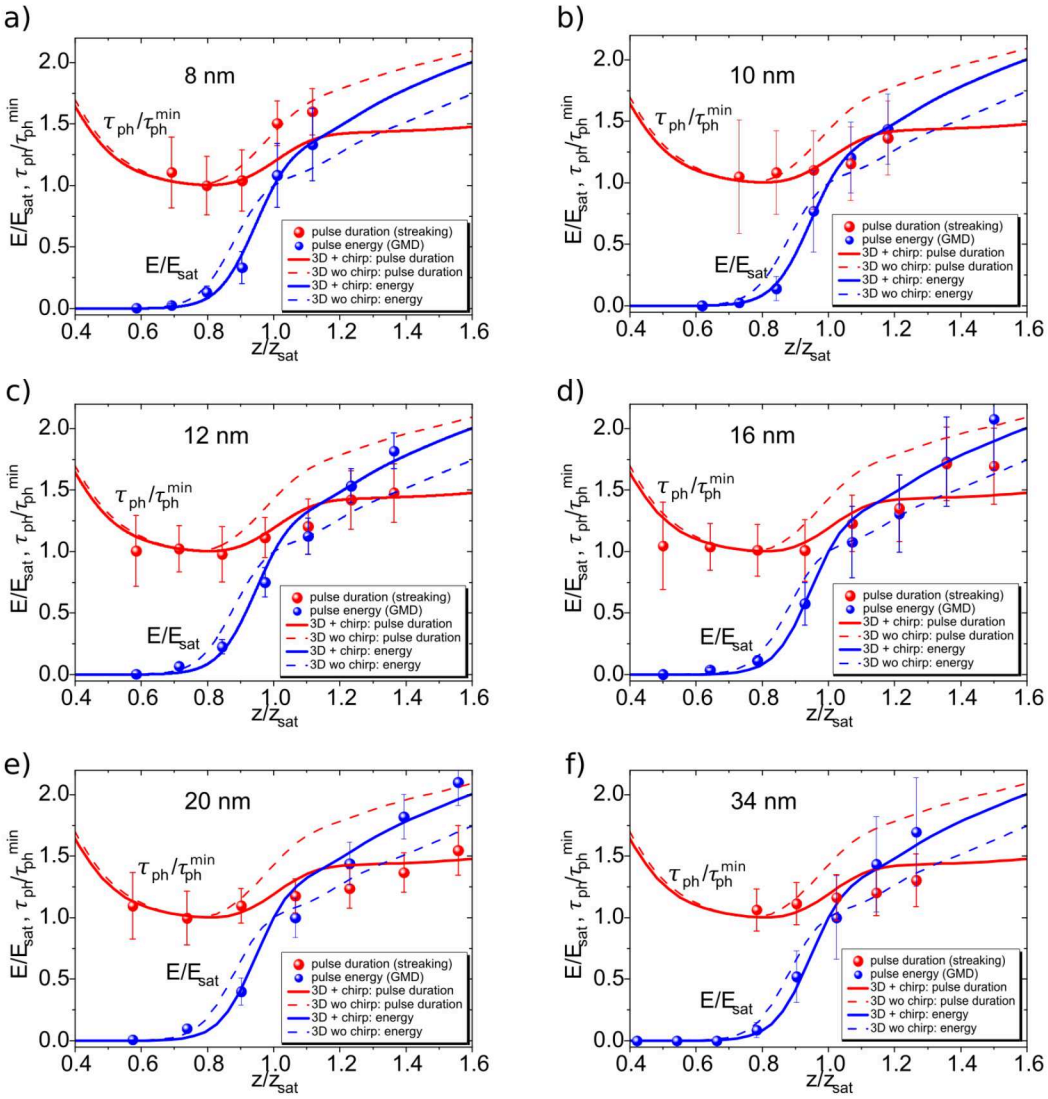

Figure 3. Evolution of the pulse duration (red circles) and pulse energy (blue circles) along the undulators. The actual undulator lengths z is normalized by the saturation length z_{sat}. The pulse energy is normalized to the saturation energy and the pulse duration to the minimum pulse duration (eq. 4). The experimental results (shown as points), represent the average over several thousand single pulse measurements, were recorded for FEL wavelengths of 8, 10, 12, 16, 20 and 34 nm and agree very well with the chirped 3D simulations (shown as red and blue solid lines). The 3D simulation without energy chirp (shown as red and blue dashed lines) are showing less agreement with the experimental data. The "error bars" denote not the experimental uncertainty but rather the width of the measured distribution induced by SASE and technical fluctuations to indicate by how much the FEL pulse energy and duration fluctuate during the measurement. (see also Fig. 4)

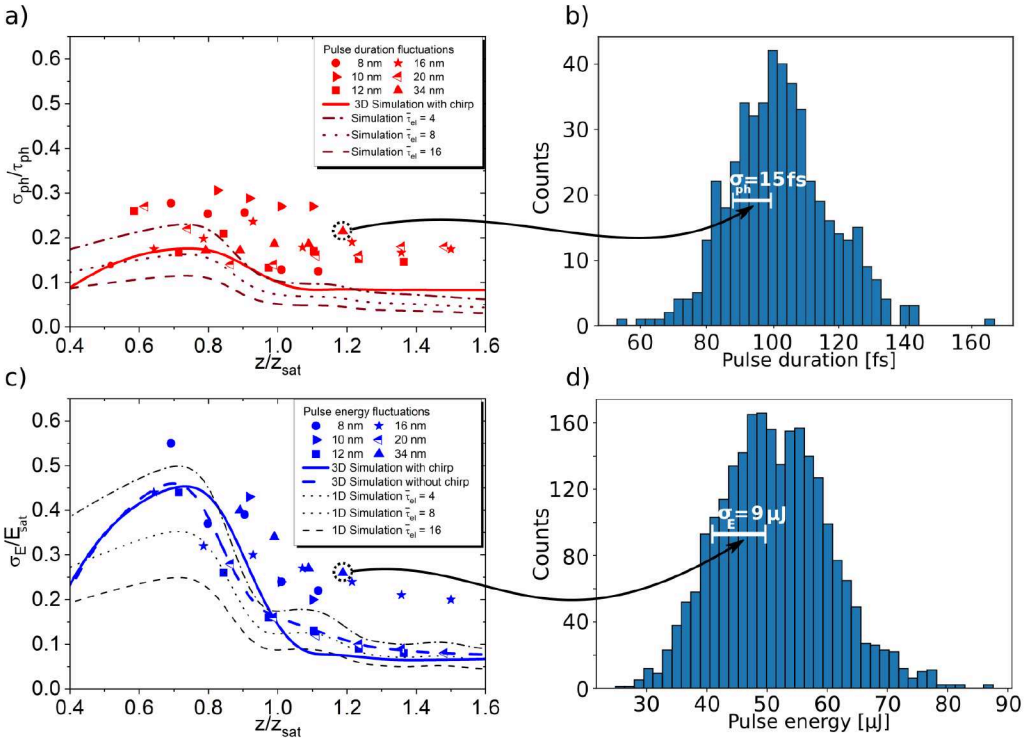

Figure 4. Shown are the fluctuations as function of the undulator coordinate z for a) the pulse duration and c) the pulse energy. For each setting several thousand FEL pulses were measured leading to a broad, Gaussian distribution as shown in b) the pulse duration and d) the pulse energy. The example histograms in b) and d) are corresponding to the data point shown with the dashed circle. The values for the fluctuations shown are the rms values of the measured pulse energies and pulse durations which are equivalent to the $1/e$ width of the histogram (for the nearly Gaussian distribution). In addition, the theoretically determined values for the fluctuations (only taking the SASE induced effects into account) are plotted for the chirped and non-chirped 3D simulation and 1D simulation for the cases of $\bar{\tau}_{el}$ =4, 8 and 16. The fact that the measured fluctuations are larger than the theoretically expected value (only for SASE) can be attributed to the measurement uncertainty and additional technical fluctuations in the accelerator as was discussed in Ref. [20].

linear regime and a small local maximum at the saturation point, which is not reproduced by the experimental data. In contrast, in the 1D simulation, the power reaches a distinct maximum saturation and grows again only for deeply saturated operation. By comparing the results from the simulation methods, the chirped 3D simulation shows a much better agreement with the experimental data and should be used as a basis for future prediction of FLASH radiation parameters.

Looking at Fig. 5, one sees a continuous power increase along the undulator length. However, as pointed out in Ref. [14,15,35], considering the spatial and spectral properties of the FEL beam it turns out that the maximum brilliance of the radiation is rather achieved in the very beginning of the nonlinear regime. Thus, for experiments that need the highest possible photon densities on the target it may be beneficial to work close to the saturation point at $z/z_{sat} \sim 1$. Since neither spectral nor spatial measurements have been performed in this study we can not test this statement experimentally.

Comparing the FEL parameters (see table 1) from the data shown in Fig. 3 we observed that for the same FEL settings (8 nm, 12 nm, 16 nm and 10 nm, 20 nm respectively), the achievable saturation energy E_{sat} increases for longer wavelength [11,36]. The minimal pulse duration ($\tau_{min}(FWHM)$) also increases slightly while the needed number of undulators to achieve saturation (z_{sat}) decreases. Plotting the saturation length as a function of the FEL wavelength together with the results from the chirped 3D simulation (Fig. 5 b) show a good agreement. This again points out that the chirped 3D simulation can be used to

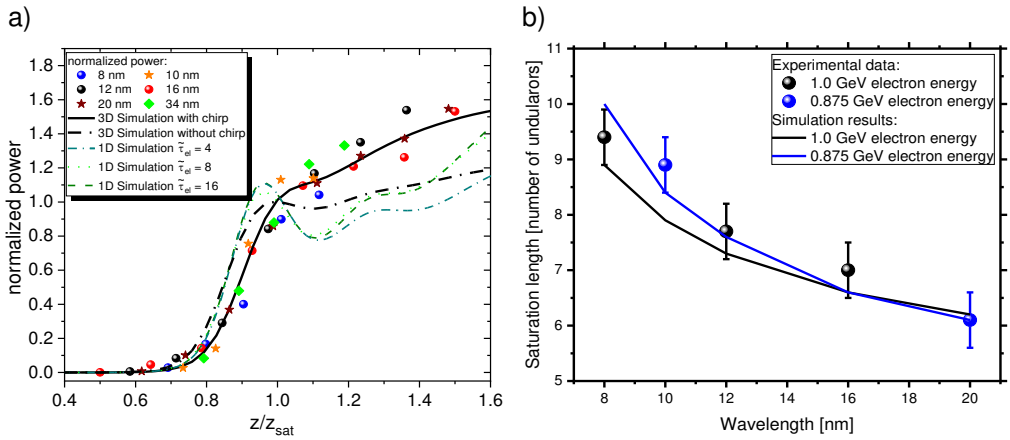

Figure 5. a) Development of the power (pulse energy divided by pulse duration), along the undulators for different pulse durations. The chirped 3D model agrees significantly better with the experimental data as compared to the non-chirped 3D model, while the oscillatory behavior predicted by the 1D model is not reproduced at all. b) The measured as well as the simulated (3D model with chirp) saturation length is plotted as function of the FEL wavelength for two different FEL setups. Error bars are estimated as ± 0.5 undulators from the analysis. The electron bunch energy for the 34 nm measurement was much smaller than for the other measurements, thus it is not included in the plot.

reliably predict FLASH2 radiation parameters despite the different experimental settings (different electron energies, undulator gaps and tuning).

5. Conclusion

We investigated the impact of the undulator length on the FEL pulse duration and pulse energy and their fluctuations for six different FEL wavelengths. We compared the simulation results from chirped and non-chirped 3D FEL simulations with 1D FEL simulations. The chirp strengths was chosen such, that the typical spectral widths ($\sim 1\%$) observed at FLASH was matched. Comparing the experimental results measured for different FEL setups with various simulation models we find a compelling agreement with the chirped 3D model even if the FEL parameters deviate significantly between measurement and simulation. This indicates that the result does not depend strongly on the particular FEL setting. The features predicted by the 1D model and the non-chirped 3D model could not be reproduced. In contrast the chirped 3D simulation results describe the behavior of the pulse energy and pulse duration rather accurately for FLASH and can be well used as input for future experiments or comparison to measurements.

Author Contributions: Measurements, M.B., S.D., R.I. and I.B.; Simulation, M.Y.; writing—original draft preparation, M.B. and S.D.; writing—review and editing, M.B., S.D., R.I., I.B. and M.Y. All authors have read and agreed to the published version of the manuscript.

Funding: This research was funded by Deutsche Forschungsgemeinschaft (DFG, German Research Foundation) grant number 491245950.

Institutional Review Board Statement: Not applicable.

Informed Consent Statement: Not applicable.

Data Availability Statement: The data presented in this study are available on request from the corresponding author.

Acknowledgments: We want to acknowledge Franz Kärtner, Mikhail Pergament, Anne-Laure Calendron, Joachim Meier, Martin Kellert and Simon Reuter for providing and maintaining our regenerative amplifier. We want to thank the DESY Synchronization group (in particular Sebastian Schulz) for providing an excellent synchronization of our laser. We would like to acknowledge Ulrike for useful

discussions and suggestions for improving this article. We also thank the FLASH operators for helpful discussions and fulfilling our special wishes during our beamtimes, in particular Juliane Rönsch-Schulenburg.

Conflicts of Interest: The authors declare no conflict of interest.

References

1. Saldin, E. L.; Schneidmiller, E. A.; Yurkov, M. V. Self-amplified spontaneous emission FEL with energy-chirped electron beam and its application for generation of attosecond x-ray pulses. *Phys. Rev. ST Accel. Beams* **2006**, *9*, 050702.
2. Saldin, E. L.; Schneidmiller, E. A.; Yurkov, M. V. Statistical properties of radiation from VUV and X-ray free electron laser. *Opt. Commun.* **1998**, *148*, 383-403.
3. Behrens, C.; Gerasimova, N.; Gerth, Ch.; Schmidt, B.; Schneidmiller, E. A.; Serkez, S.; Wesch, S.; Yurkov, M. V. Constraints on photon pulse duration from longitudinal electron beam diagnostics at a soft x-ray free-electron laser. *Phys. Rev. ST Accel. Beams* **2012**, *15*, 030707.
4. Lutman, A. A.; Ding, Y.; Feng, Y.; Huang, Z.; Messerschmidt, M.; Wu, J.; Krzywinski, J. Femtosecond x-ray free electron laser pulse duration measurement from spectral correlation function. *Phys. Rev. ST Accel. Beams* **2012**, *15*, 030705.
5. Ackermann, W.; Asova, G.; Ayvazyan, V.; et al. Operation of a Free Electron Laser in the Wavelength Range from the Extreme Ultraviolet to the Water Window. *Nature Photonics* **2007**, *1*, 336–342.
6. Emma, P.; Akre, R.; Arthur, J; et al. First lasing and operation of an ångstrom-wavelength free-electron laser. *Nature Photon* **2010**, *4*, 641–647.
7. Ishikawa, T., Aoyagi, H., Asaka, T; et al. A compact X-ray free-electron laser emitting in the sub-ångström region. *Nature Photon* **2012**, *6*, 540–544.
8. Decking, W.; Abeghyan, S.; Abramian, P; et al. A MHz-repetition-rate hard X-ray free-electron laser driven by a superconducting linear accelerator. *Nature Photon* **2020**, *14*, 391–397.
9. Milne, C.J.; Schietinger, T.; Aiba, M.; Alarcon, A.; Alex, J.; et al. SwissFEL: The Swiss X-ray Free Electron Laser. *Appl. Sci.* **2017**, *7*, 720.
10. Ding, T.; Rebholz, M.; Aufleger, L.; Hartmann, M.; et al. A new powerful source for coherent VUV radiation: Demonstration of exponential growth and saturation at the TTF free-electron laser. *Eur. Phys. J. D* **2002**, *20*, 149–156.
11. Faatz, B.; Plönjes, E.; Ackermann, S.; Agababyan, A.; Asgekar, V.; et al. Simultaneous operation of two soft x-ray free-electron lasers driven by one linear accelerator. *New Journal of Physics* **2016**, *18*, 062002.
12. Saldin, E. L.; Schneidmiller, E. A.; Yurkov, M. V. FAST: a three-dimensional time-dependent FEL simulation code. *Nuclear Instruments and Methods in Physics Research Section A: Accelerators, Spectrometers, Detectors and Associated Equipment,* **1999**, *429*, 233-237.
13. Saldin, E. L.; Schneidmiller, E. A.; Yurkov, M. V. *The Physics of Free Electron Lasers.*, 3rd ed.; Springer-Verlag: Berlin, Germany, 1999.
14. Saldin, E. L.; Schneidmiller, E. A.; Yurkov, M. V. Coherence properties of the radiation from X-ray free electron laser. *Opt. Commun.* **2008**, *281*, 1179-1188.
15. E. L.; Schneidmiller, E. A.; Yurkov, M. V. Coherence Properties of the Radiation from X-ray Free Electron Lasers. *Proceedings of the CAS-CERN Accelerator School on Free Electron Lasers and Energy Recovery Linacs* **2018**, *1*.
16. Bonifacio, R.; Pellegrini, C.; Narducci, L. M. Collective instabilities and high-gain regime in a free electron laser. *Opt. Commun.* **1984**, *50*, 373.
17. Bonifacio, R.; De Salvo, L.; Pierini, P.; Piovella, N.; Pellegrini, C. Spectrum, temporal structure, and fluctuations in a high-gain free-electron laser starting from noise. *Phys. Rev. Lett.* **1994**, *73*, 70-73.
18. E. L.; Schneidmiller, E. A.; Yurkov, M. V. Application of statistical methods for measurements of the coherence properties of the radiation from SASE FEL. *Proc. IPAC2016* **2016**, MOPOW013.
19. Saldin, E. L.; Schneidmiller, E. A.; Yurkov, M. V. Statistical properties of radiation from SASE FEL driven by short electron bunches. *Nuclear Instruments and Methods in Physics Research Section A: Accelerators, Spectrometers, Detectors and Associated Equipment* **2003**, *1–2*, 101-105.
20. Bermudez, I.; Düsterer, S.; Ivanov, I.; Liu, J.; Brenner, G.; Rönsch-Schulenburg, J.; Czwalinna, M.; Yurkov, M. Study of temporal, spectral, arrival time and energy fluctuations of SASE FEL pulses. *Optics Express* **2021**, *29*, 10491-10508.
21. Zagorodnov, I.; Dohlus, M. Semianalytical modeling of multistage bunch compression with collective effects. *Phys. Rev. ST Accel. Beams* **2011**, *14*, 014403.
22. Mayer, D.; Lever, F.; Picconi, D.; et al. Following excited-state chemical shifts in molecular ultrafast x-ray photoelectron spectroscopy. *Nat. Commun.* **2022**, *13*, 198.
23. von Korff Schmising, C.;Willems, F.; Sharma, S.; Yao, K.; Borchert, M.; et al. Element-Specific Magnetization Dynamics of Complex Magnetic Systems Probed by Ultrafast Magneto-Optical Spectroscopy. *Appl. Sci.* **2022**, *10*, 7580.
24. Gerth, C.; Brenner, G.; Caselle, M.; Dusterer, S.; Haack, D.; et al. Linear array detector for online diagnostics of spectral distributions at MHz repetition rates. *J. Synchrotron Rad.* **2019**, *26*, 1514 - 1522.
25. Ding, T.; Rebholz, M.; Aufleger, L.; Hartmann, M.; et al. Measuring the frequency chirp of extreme-ultraviolet free-electron laser pulses by transient absorption spectroscopy. *Nat. Commun.* **2021**, *12*, 643.

26. Frühling, U.; Wieland, M.; Gensch, M.; et al. Single-shot terahertz-field-driven X-ray streak camera. *Nature Photonics* **2009**, *3*, 523-528.
27. Grguraš, I.; Maier, A.; Behrens, C.; et al. Ultrafast X-ray pulse characterization at free-electron lasers. *Nature Photonics* **2012**, *6*, 852-857.
28. Frühling, U. Light field streaking for FELs. *J. Phys. B: At. Mol. Opt. Phys.* **2011**, *44*, 243001.
29. Ivanov, R.; Bermudez, I.; Bidhendi, M.; Brachmanski, M.; Kreis, S.; Bonfigt, S.; Degenhardt, M.; Düsterer, S. Photon diagnostic beamline FL21 at FLASH. *J. Synchrotron Rad.* 2022, *submitted*.
30. Ivanov, R.; Liu, J.; Brenner, G.; Brachmanski, M.; Düsterer, S. FLASH free-electron laser single-shot temporal diagnostic: terahertz-field-driven streaking. *J. Synchrotron Rad.* **2018**, *25*, 26.
31. Ivanov, R.; Bermudez, I.; Liu, J.; Brenner, G.; Rönsch-Schulenburg, J.; Kurdi, G.; et al. Single-shot temporal characterization of XUV pulses with duration from $\sim$ 10 fs to $\sim$ 350 fs at FLASH. *J. Phys. B.* **2020**, *53* 184004.
32. Tiedtke, K.; Azima, A.; von Bargen, N.; Bittner, L.; Bonfigt, S.; Düsterer, S.; et al. The soft x-ray free-electron laser FLASH at DESY: beamlines, diagnostics and end-stations. *New J. Phys.* **2009**, *11*, 023029.
33. Roling, S.; Siemer, B.; Wöstmann, M.; Zacharias, H.; Mitzner, R.; Singer, A.; Tiedtke, K.; Vartanyants, I.A. Temporal and spatial coherence properties of free-electron-laser pulses in the extreme ultraviolet regime. *Phys. Rev. ST Accel. Beams* **2011**, *14*, 080701.
34. Tiedtke, K.; Feldhaus, J.; Hahn, U.; Jastrow, U.; Nunez, T.; et al. Gas detectors for x-ray lasers. *J. Appl. Phys.* **2008**, *103*, 094511.
35. Saldin, E. L.; Schneidmiller, E. A.; Yurkov, M. V. Statistical and coherence properties of radiation from x-ray free-electron lasers. *New Journal of Physics* **2010**, *12*, 035010.
36. Faatz, B.; Braune, M.; Hensler, O.; Honkavaara, K.; Kammering, R.; Kuhlmann, M.; et al. The FLASH Facility: Advanced Options for FLASH2 and Future Perspectives. *Appl. Sci.* **2017**, *7*, 1114.